



ISSN: 0067-2904

## Hydrothermal Process to Prepare Novel Phase Titanium Sub-Oxide $Ti_6O_{11}$ from Nano Rutile Titanium Dioxide Particles with Different Autodave Reactors

Mohanad Q.Fahem<sup>1\*</sup>, Thamir A.A. Hassan<sup>2</sup>

<sup>1</sup>Department of Physics, College of Science, University of Baghdad, Baghdad, Iraq

<sup>2</sup>Alkarkh University of Science, Baghdad-Iraq, Baghdad, Iraq

Received: 8/1/2022

Accepted: 17/2/2022

Published: 30/11/2022

### Abstract

Hydrothermal process method using different dimensions reactors with volume 100 ml (homemade) was employed to prepare titanium sub-oxide  $Ti_6O_{11}$ , where one gram of  $TiO_2$  nanoparticles 30-50 nm and 3M (20 ml) of NaOH as suspension was used. The samples are characterized using X-ray diffraction, Raman spectroscopy, and Field Emission Scanning Electron Microscopy (FE-SEM). X-ray diffraction revealed the formation of sub-oxide titanium  $Ti_6O_{11}$  of triclinic structure with Magneli phase, when the temperature applied was 363K for 9h. While FE-SEM showed uniform hierarchical structures with planar grass-like shapes. A novel phase has been found from rutile titanium.

**Keywords:** Hydrothermal, magneli, titanium sub-oxide  $Ti_6O_{11}$ , hierarchical structure,

العملية الحرارية المائية لتحضير المرحلة الجديدة من ثاني أكسيد التيتانيوم الفرعي  
من جزيئات ثاني أكسيد التيتانيوم النانوية الروتيل بمفاعلات الأوتوكلاف مختلفة  $Ti_6O_{11}$

مهند قاسم فاهم<sup>1</sup> ، ثامر عبد الامير حسين<sup>2\*</sup>

<sup>1</sup>قسم الفيزياء، كلية العلوم، جامعة بغداد، بغداد، العراق

<sup>2</sup>جامعة الكرخ للعلوم، بغداد، العراق

### الخلاصة

تم استخدام طريقة العملية الحرارية المائية باستخدام مفاعلات ذات أبعاد مختلفة بحجم 100 مل (محلية الصنع) لتحضير أكسيد التيتانيوم الفرعي  $Ti_6O_{11}$  ، حيث تم استخدام غرام واحد من جزيئات  $TiO_2$  النانوية 30-50 نانومتر و 3 مولاري (20 مل) من هيدروكسيد الصوديوم كمعلق. تتميز العينات باستخدام حيود الأشعة السينية ، ومطياف رامان ، والمجهر الإلكتروني لمسح الانبعاث الميداني (FE-SEM). كشف حيود الأشعة السينية عن تكوين أكسيد التيتانيوم الفرعي  $Ti_6O_{11}$  لهيكل ثلاثي الميل مع طور Magneli ، عندما كانت درجة الحرارة المطبقة 363 كلفن لمدة 9 ساعات ، بينما أظهر FE-SEM هياكل هرمية موحدة بأشكال تشبه العشب المستوي. تم العثور على طور جديد من روتيل التيتانيوم.

\*Email: [President@kus.edu.iq](mailto:President@kus.edu.iq)

## 1. Introduction

The preparation of partially oxidized titanium dioxide by hydrothermal method is an important research aspect in recent times. Because of its nanostructures diverse and peculiar properties, it is used in many applications.

Crystal phase, particle size, and particle shape all influence the physical and chemical characteristics of  $\text{TiO}_2$  [1,2]. Rutile, brookite, and anatase are the three crystalline phases of  $\text{TiO}_2$ . Thermodynamically, the rutile phase is stable, but brookite and anatase are metastable [3,4]. The  $\text{TiO}_2$  anatase phase is widely considered to be the active phase in photochemical applications [5]. According to several observations in the literature, rutile  $\text{TiO}_2$  is also more active in photochemical applications than anatase  $\text{TiO}_2$  [6,7].

Magneli phases are titanium sub oxides with the general formula  $\text{Ti}_n\text{O}_{2n-1}$  ( $n$  is an integer between 4-10) [8, 9].  $\text{Ti}_n\text{O}_{2n-1}$  is a highly conductive oxide with distinct physical, chemical, and optical properties that could be employed in photo catalysis, photovoltaics, fuel cells, data storage, and energy conversion devices because of its narrow band gap [10, 11]. Magnéli [12, 13] solved the structure of  $\text{Ti}_n\text{O}_{2n-1}$  in the 1950s. Which is identical to the edge shared  $\text{TiO}_6$  octahedra chain structure, with the exception that sharing occurs in each octahedron due to Ti reduction and the consequent oxygen vacancies in  $\text{Ti}_n\text{O}_{2n-1}$  [12, 10]. Due to their outstanding conductivity and extraordinary absorptivity of visible light, the titanium–oxygen system plays a vital role in the research of a material's non-stoichiometry and is employed in a variety of applications [14]. Magneli phase has been utilized as a counter electrode in solar cells and has shown to have a greater short-circuit current density than Pt [15, 16]. Magneli phase is also corrosion resistant.

Controlling the crystallization, size, and shape of nanostructured  $\text{TiO}_2$  is crucial for fabricating materials with the desired properties, and it is a hot topic of research. [17, 18]. Although a direct correlation between surface and physicochemical qualities is not always possible, it has been shown that  $\text{TiO}_2$  activity is influenced by crystal structure, surface condition, and size distribution [19, 20].

Because differences in Raman spectra with the decrease of particles size may easily be identified, Raman spectroscopy is considered as a valuable tool for investigating the structural features of nanoparticles [21,22]. This technique provides valuable information on the surface and the effects of nanoparticles' finite size as new bands can appear or vanish, as particle size decreases due to an increase in the surface-to-volume ratio, or a broadening band can appear. Campbell and Fauchet reported that grain size effects produce large shifts and broadening of the Raman spectrum [23].

## 2. Materiel and Methods

Three stainless steel reactors (A, B and C) of 100ml capacity with dimensions [diameter: height]: A (55mm: 130mm), B (65mm: 100mm) and C (75mm: 80mm) (as shown in Figure 1) were designed and fabricated in our laboratory. Each reactor is composed of an inner Teflon autoclave positioned inside a stainless steel cylinder that can be tightly closed with a screwed cover. The cylinder acts as a furnace as it is surrounded externally by a heater of 300W power, and is supplied with a thermocouple for temperature control. Figure 2-a shows the three fabricated reactors of the different dimensions. Figure 2-b shows the basic components of the reactors autoclaves used.

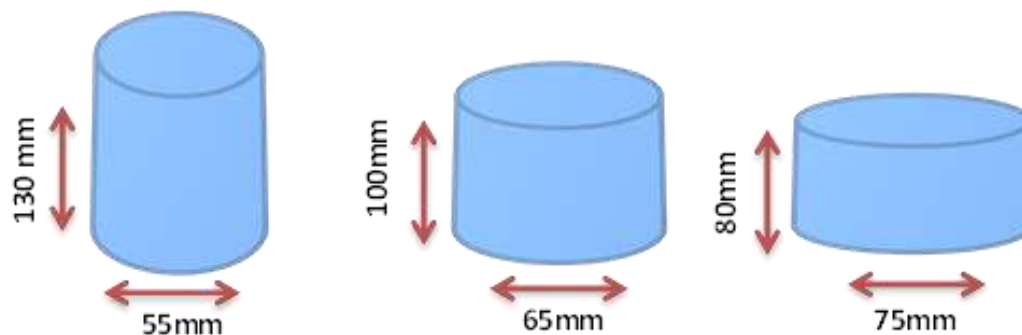


**Figure 1:** Schematic diagram showing the dimensions of the three autoclave reactors.

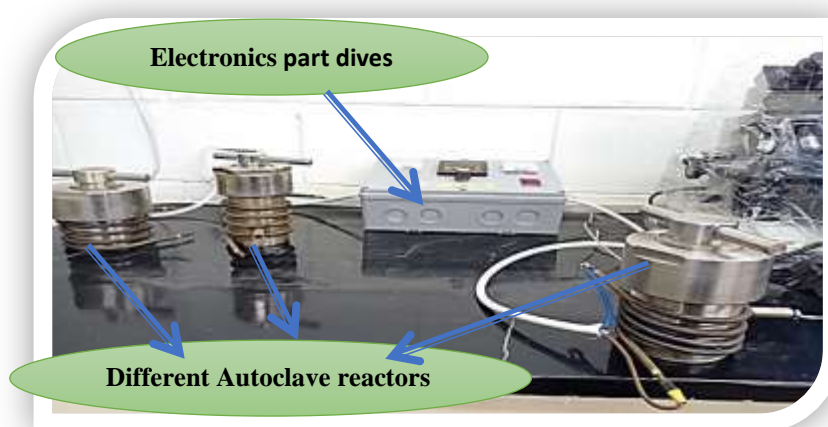


**Figure 2 a:** A picture showing the two part of the hydrothermal method

One gram of  $\text{TiO}_2$  nanoparticles rutile (Purchased from Hongwu international Group) was added to 20ml of 3M NaOH at room temperature with continuous stirring until its colour changed to white, a process that required 20 minutes at the most. 20ml of the white suspension was put inside each autoclave reactor and heated to a temperature of 363k for 9 hours to prepare nano titanium sub oxide with Magneli phase. The product of the reaction in the autoclaves reactors was washed several times with ethanol and distilled water, dried for 30 min and filtered by Büchner funnel using filter paper (of pore size=200nm). Furthermore, the product was heated at 523k for 1 h for homogeneity and to remove any residual organic materials.

Structural properties of the prepared samples were studied by X-ray diffraction (XRD) analysis (Analytical X' Pert Pro/ United Kingdom, Raman spectroscopy (HORIBA XploRA PLUS/ Japan). In addition, the surface morphology of the prepared samples was studied with field emission scanning electron microscope (EBSD Instrument: ZEISS SIGMA VP./ Germany).



**Figure 2 b:** The different parts of the stainless steel autoclave.

## 2. Results and discussion

Titanium sub oxide prepared from Rutile titanium dioxide by hydrothermal method was characterized by XRD. Figure 3 shows the XRD patterns of the Ti sub oxide prepared in the three reactors (A, B and C). The crystalline planes were found to be: for reactor A at (002), (10-1), (020), (02,12), (21,13), (1-1,10), (202) and (033) for  $2\theta$  ( $10^{\circ}.10^{\circ}$ ,  $30^{\circ}.10^{\circ}$ ,  $37^{\circ}.96^{\circ}$ ,  $39^{\circ}.94^{\circ}$ ,  $41^{\circ}.19^{\circ}$ ,  $44^{\circ}.31^{\circ}$ ,  $46^{\circ}.52^{\circ}$  and  $48^{\circ}.18^{\circ}$ ), respectively, for reactor B at (002), (10-1), (020), (02,12), (21,13), (1-1,10), (202) and (033) for  $2\theta$  ( $10.01^{\circ}$ ,  $30.10^{\circ}$ ,  $38^{\circ}.02^{\circ}$ ,  $39^{\circ}.97^{\circ}$ ,  $41^{\circ}.25^{\circ}$ ,  $44^{\circ}.57^{\circ}$ ,  $46^{\circ}.52^{\circ}$  and  $48^{\circ}.32^{\circ}$ ), respectively and for reactor C at (1 0 -1), (0 2 0), (0 2, 12), (2 1, 13), (1 -1, 10), (2 0 2) and (0 3 3) for  $2\theta$  ( $30^{\circ}.21^{\circ}$ ,  $38^{\circ}.07^{\circ}$ ,  $40^{\circ}.00^{\circ}$ ,  $41^{\circ}.51^{\circ}$ ,  $44^{\circ}.63^{\circ}$ ,  $46^{\circ}.69^{\circ}$  and  $48^{\circ}.32^{\circ}$ ) respectively. This result is compatible with Joint Committee on Powder Diffraction Standards (JCPDS) card No:96-100-8196. It can be noticed that the XRD pattern of Ti sub oxide prepared in reactor C revealed the disappearance of the crystal plane (0 0 2). Scherrer equation was used to calculate the average crystalline size (C.S) of Ti sub oxide which were (16.7nm, 16.06nm and 19.7 nm), from reactors A, B and C, respectively (as shown in Figure 4 and the values are tabulated in Table1). The difference in the surface area of each reactor causes a difference in the crystal size of the prepared sample, as it is believed that the difference in the surface area is the cause of a difference in the crystal growth of the resulting sample due to the increase in the speed of movement of the suspended particles during the reaction inside the reactor by increasing the surface area of the liquid.

Applying heat and pressure to titanium suspension in the reactors caused the formation of titanium and oxygen of imbalance ratios. The production of sub- oxide titanium with the Magneli phase was specific to autoclave reactors A and B. This was confirmed by Raman spectroscopy.

Stabilized Magneli phase were materials characterized by high corrosion resistance in acidic and basic solutions, electrical conductivity and electrochemical stability are both high [8].

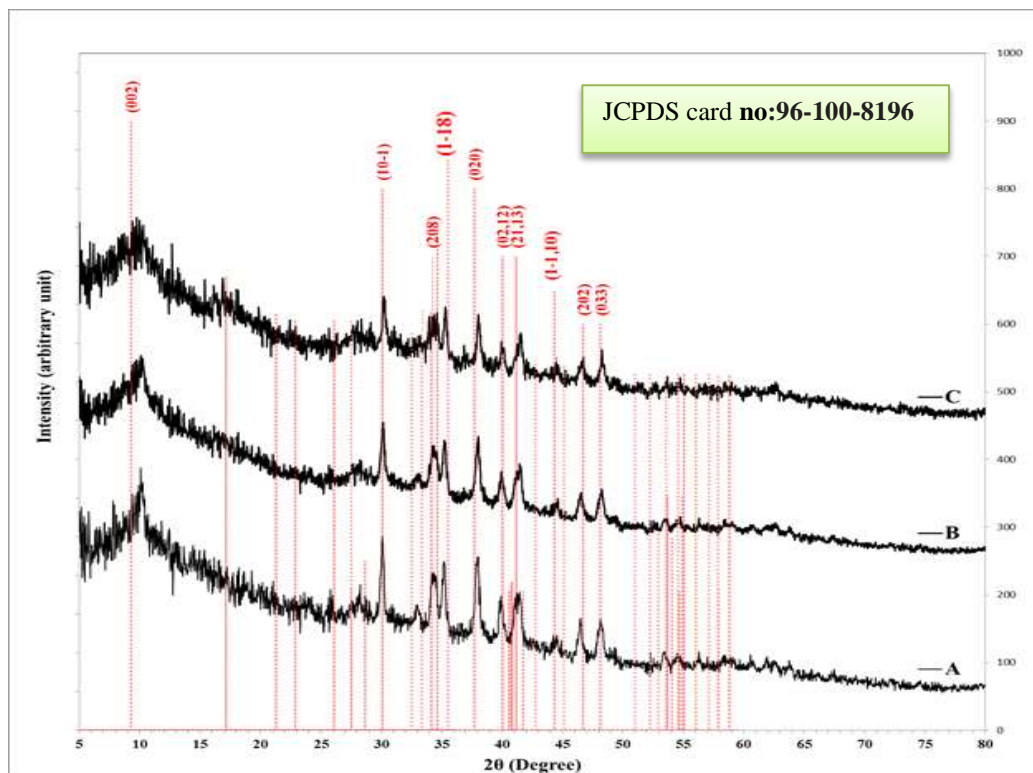


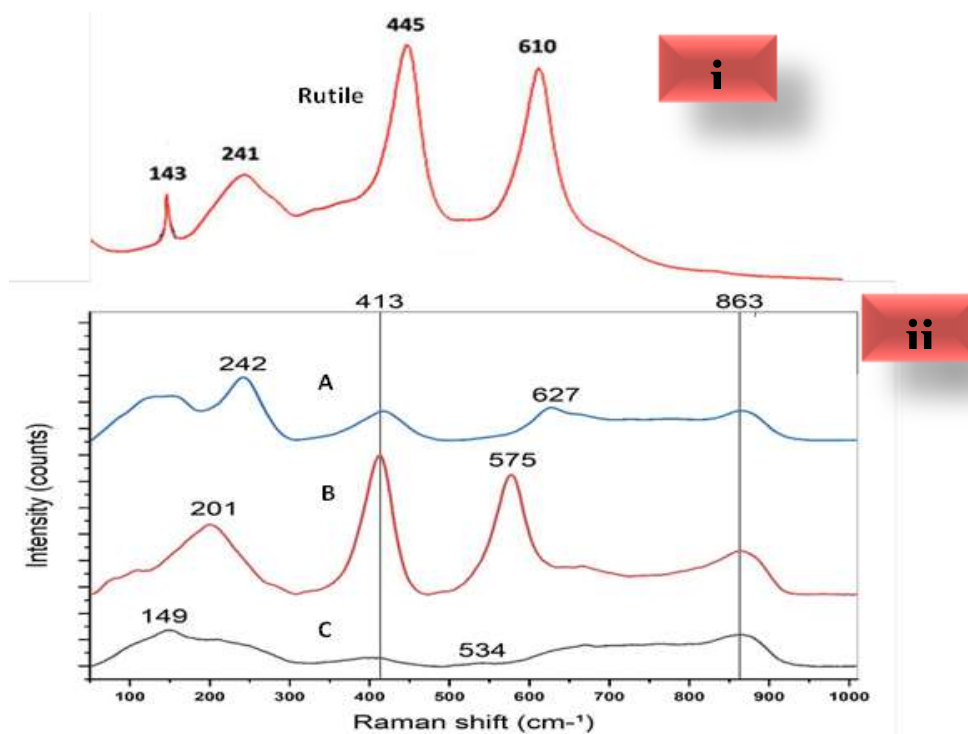
**Figure 3:** XRD pattern for samples after restructured by the hydrothermal method at 90 °C for 9 h using different autoclave reactor (A), (B) and (C)

Comparing the Raman spectra of rutile titanium dioxide with those of the samples from the three reactors autoclaves, as illustrated in Figure 5, revealed that the product of the reaction of reactor B shows two prominent Raman lines at  $413$  and  $575\text{cm}^{-1}$  comparable to the rutile Raman lines at  $446.6$  and  $609.8\text{cm}^{-1}$ . The shift of the position of Raman lines is due to a decrease in the ratio of oxygen indicating the presence of titanium sub-oxide. Hence, these results confirmed the formation of titanium sub-oxide with Magneli phase ( $\text{Ti}_6\text{O}_{11}$  triclinic). Therefore, the dimensions of autoclave reactor B (65mm: 100mm) are the best for the formation of Magneli phase  $\text{Ti}_6\text{O}_{11}$  triclinic.

The absence of these two Raman lines in the spectra related to autoclave reactor C and reactor A indicates a decrease in the ratios of oxygen bonds with titanium, which could not lead to the formation of the Magneli phase. These results agree with those of Parker and Siegel [24].

**Table 1:** XRD parameters for the TiO<sub>2</sub> NPs after restructured by hydrothermal at 363k for 9 h using different autoclave reactor (A), (B) and (C).

Sample	2θ (Deg.)	FWHM (Deg.)	d <sub>hkl</sub> Exp. (Å)	C.S (nm)	d <sub>hkl</sub> Std.(Å)	Hkl
A	10.10	0.70	8.76	11.41	9.54	(002)
	30.10	0.32	2.97	25.69	2.97	(10-1)
	37.96	0.41	2.37	20.61	2.38	(020)
	39.94	0.35	2.26	24.20	2.25	(0212)
	41.19	0.67	2.19	12.67	2.19	(2113)
	44.31	0.52	2.04	16.37	2.04	(1-110)
	46.52	0.58	1.95	14.85	1.94	(202)
B	48.18	0.61	1.89	14.23	1.89	(033)
	10.01	0.99	8.83	8.06	9.54	(002)
	30.10	0.44	2.97	18.84	2.97	(10-1)
	38.02	0.47	2.37	18.04	2.38	(020)
	39.97	0.47	2.25	18.15	2.25	(0212)
	41.25	0.76	2.19	11.21	2.19	(2113)
	44.57	0.41	2.03	21.06	2.04	(1-110)
C	46.52	0.58	1.95	14.85	1.94	(202)
	48.32	0.58	1.88	14.95	1.89	(033)
	30.21	0.44	2.96	18.84	2.97	(10-1)
	38.07	0.35	2.36	24.05	2.38	(020)
	40.00	0.44	2.25	19.35	2.25	(0212)
	41.51	0.47	2.17	18.23	2.19	(2113)
	44.63	0.41	2.03	21.07	2.04	(1-110)
46.69	0.61	1.94	14.15	1.94	(202)	
48.32	0.44	1.88	19.93	1.89	(033)	

**Figure 4:** Raman spectra of (i) reference (Rutile), and (ii) for samples after restructured by hydrothermal at 90 °C for 9 h using different autoclave reactor (A), (B) and (C).



**Figure 5:** crystallite size of samples in different autoclave reactor (A), (B) and (C) from XRD analysis according to Scherrer equation.

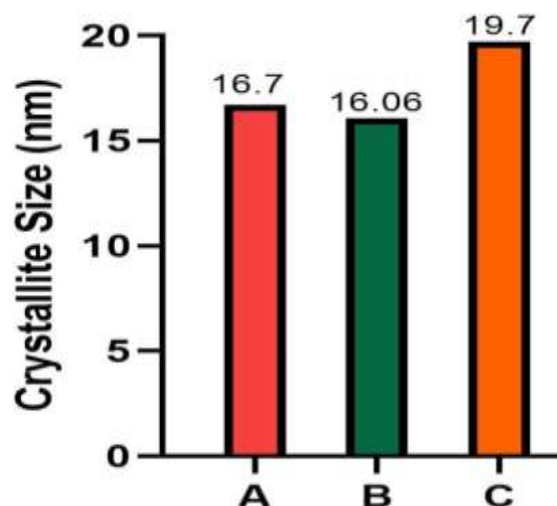


**Figure 6:** FL- SEM images two size of the  $\text{Ti}_6\text{O}_{11}$  samples prepared by hydrothermal method using different autoclave reactor (A), (B) and (C) of hierarchical nanostructures

The SEM images (Figure 6) shows the topography and the morphology of  $\text{Ti}_6\text{O}_{11}$  with Magneli phase, the chemical product of the reactions in (A), (B) and (C) autoclave reactors. They show uniform hierarchical nanostructures with other morphology types such as planar grass-like shapes.

The products ( $\text{Ti}_6\text{O}_{11}$ ) with hierarchical nanostructures have many important applications such as in support of the Pt catalyst in solar cells, organic degradation, coatings and supports in various electronic and optoelectronic devices. Titanium sub-oxides are expected to become important materials in the future [14] because of its excellent conductivity and excellent absorption of visible light [26]. And the hierarchical nanostructures  $\text{Ti}_6\text{O}_{11}$  are also very important in various applications, because of its huge surface area to volume ratio [25].

#### 4. Conclusions

The change in the dimensions of the reactors of the same capacity has caused variable forms of the reaction due to the different heat distribution and the change in reactor pressure. This resulted in the formation of type  $\text{Ti}_6\text{O}_{11}$  sub oxide titanium with **Magneli** phase. Because of the re-formation of oxygen bonds (Ti-O) in titanium for rutile  $\text{TiO}_2$  in the reactor, type  $\text{Ti}_6\text{O}_{11}$  sub oxide titanium with **Magneli** phase of hierarchical nanostructures was produced.

#### References

- [1] Z. Zhang., C.C. Wang, R. Zakaria, and J.Y. Ying, "Role of particle size in nanocrystalline  $\text{TiO}_2$ -based photocatalysts." *The Journal of Physical Chemistry B*, 102(52), pp.10871-10878,1998.
- [2] Z. Tan, K. Sato, S. Takami, C. Numako, M. Umetsu, K. Soga, M. Nakayama, R.Sasaki, T. Tanaka, C. Ogino, A. Kondo, K. Yamamoto, T. Hashishin, S. Ohara, "Particle size for photocatalytic activity of anatase  $\text{TiO}_2$  nanosheets with highly exposed {001} facets". *RSC advances*, 3(42), pp.19268-19271, 2013.
- [3] G. J. Wilson, A. S. Matijasevich, D. R. G. Mitchell, J. C. Schulz and G. D. Will "Modification of  $\text{TiO}_2$  for enhanced surface properties: finite Ostwald ripening by a microwave hydrothermal process" *Langmuir*, 22(5), 2016-2027, 2006.
- [4] Y. Hu, H. L. Tsai, C.L. Huang, "Effect of brookite phase on the anatase–rutile transition in titania nanoparticles." *European Ceramic Society* 23, no. 5, 691-696,2003.
- [5] Wu W Q, Lei B X, H. S. Rao, Xu Y F, Wang Y F, Su C Y, Su C.Y. and D.B. Kuang "Hydrothermal fabrication of hierarchically anatase  $\text{TiO}_2$  nanowire arrays on FTO glass for dye-sensitized solar cells." *Scientific reports*, 3(1), 1-7, 2013.

- [6] A. M. Selman and Z. Hassan "Growth and characterization of rutile TiO<sub>2</sub> nanorods on various substrates with fabricated fast-response metal–semiconductor–metal UV detector based on Si substrate." *Superlattices and Microstructures*, 83, pp.549-564,2015.
- [7] Z. Zhang, J. Li, X. Wang, J. Qin, W. Shi, Y. Liu ,H. Gao , Y. Mao, "Growth of Zr/N-codoped TiO<sub>2</sub> nanorod arrays for enhanced photovoltaic performance of perovskite solar cells." *RSC advances*, 7(22), 13325-13330, 2017.
- [8] L. Liborio and N. Harrison, " Thermodynamics of oxygen defective Magnéli phases in rutile: A first-principles study." *Physical Review B* 77, no. 10, pp.104104, 2008.
- [9] Walsh, F. C., and R. G. A. Wills. "The continuing development of Magnéli phase titanium sub-oxides and Ebonex (R) electrodes." *Electrochimica Acta* 55(22), pp.6342,2010.
- [10] D. Portehault, V. Maneeratana, C. Candolfi, N. Oeschler, I. Veremchuk, Y. Grin, C. Sanchez and M. Antonietti, , "Facile general route toward tunable magnéli nanostructures and their use as thermoelectric metal oxide/carbon nanocomposites." *ACS nano*, 5(11), pp.9052-9061,2011.
- [11] S.Tominaka, Y. Tsujimoto, Y. Matsushita, K. Yamaura, "Synthesis of nanostructured reduced titanium oxide: crystal structure transformation maintaining nanomorphology." *Angewandte Chemie*, 123(32), pp.7556-7559, 2011.
- [12] S. Andersson, B. Collen, G. Kruuse, U. Kuylenstierna, A. Magnéli, H. Pestmalis, S., Andersson, S. T. E. N. Åsbrink, "Identification of titanium oxides by X-ray powder patterns." *Acta Chem. Scand. B* 11, 1957.
- [13] S. Andersson, B. Collen, U. Kuylenstierna, A. Magnéli, "Phase analysis studies on the titanium-oxygen system." *Acta Chem. Scand.* 11(10), pp.1641-1652,1957.
- [14] B. Xu, H. Y. Sohn, Y. Mohassab, Y. Lan, "Structures, preparation and applications of titanium sub-oxides." *RSC advances*, 6(83), pp.79706-79722, 2016.
- [15] Y. Suzuki, M.Takemoto, "Dye sensitized solar cell using Ti<sub>4</sub>O<sub>7</sub> as a counter electrode material." *Transactions of the Materials Research Society of Japan* , 39(3), 349, 2014.
- [16] L. Xu, Y. Zhao, G. Long, Y. Wang, J. Zhao, D. Li, and Q. Zhang, "Synthesis, structure, physical properties and OLED application of pyrazine–triphenylamine fused conjugated compounds." *RSC advances*, 5(77), pp.63080-63086, 2015.
- [17] H. Yin, Y. Wada, T. Kitamura, S. Kambe, S. Murasawa, H. Mori, T. Sakata, S.Yanagida, "Hydrothermal synthesis of nanosized anatase and rutile TiO<sub>2</sub> using amorphous phase TiO<sub>2</sub>." *Journal of Materials Chemistry*, 11(6), pp.1694-1703, 2001.
- [18] C.T. Dinh, T.D. Nguyen, F. Kleitz, T.O. Do, "Shape-controlled synthesis of highly crystalline titania nanocrystals." *ACS nano*, 3(11), 3737-3743, 2009.
- [19] H. Harada, T. Ueda "Photocatalytic activity of ultra-fine rutile in methanol-water solution and dependence of activity on particle size." *Chemical physics letters*, 106(3), pp.229-231, 1984.
- [20] C. Y. Xu, P. X. Zhang and L. Yan. "Blue shift of Raman peak from coated TiO<sub>2</sub> nanoparticles." *Journal of Raman spectroscopy*, 32(10), pp.862-865, 2001.
- [21] G. Scamarcio , M. Lugara´, D. Manno , "Size-dependent lattice contraction in CdS 1– x Se x nanocrystals embedded in glass observed by Raman scattering." *Physical Review B*, 45(23), 13792, 1992.
- [22] de Paula, A. M.; Barbosa, L. C.; Cruz, C. H. B.; Alves, O. L.; Sanjurjo, J. A.; Cesar, C. L "Size effects on the phonon spectra of quantum dots in CdTe-doped glasses." *Applied Physics Letters*. 69(3), 357, 1996.
- [23] I.H. Campbell, P.M. Fauchet, "The effects of microcrystal size and shape on the one phonon Raman spectra of crystalline semiconductors." *Solid State Communications*, 58(10), 739-741, 1986.
- [24] J.C. Parker, R.W. Siegel, "Calibration of the Raman spectrum to the oxygen stoichiometry of nanophase TiO<sub>2</sub>." *Applied Physics Letters*, 57(9), 943-945,1990.
- [25] X. Li, Y. Liu and J. Ye "Investigation of fabrication of Ti<sub>4</sub>O<sub>7</sub> by carbothermal reduction in argon atmosphere and vacuum." *Journal of Materials Science: Materials in Electronics*, 27(4), 3683-3692, 2016.
- [26] M.maria A. S., N. kumaresan1, K. ramamurthi and K. sethuraman, "Development of pure rutile  $\text{TiO}_2$  and Magneli titanium sub-oxide microstructures over titanium oxide-seeded glass substrates using surfactant-free hydrothermal process." *Bulletin of Materials Science*, 42(3), 1-8,2019.